*Materials Transactions*, Vol. 43, No. 11 (2002) pp. 2885 to 2889


# Mössbauer Study on the Crystallization Process of $\alpha$-Fe/$Nd_2Fe_{14}B$ type Nanocomposite Magnet Alloy

Minoru Yamasaki[1], Masaaki Hamano[2] and Takayuki Kobayashi[3]

[1]*Toda Kogyo Corporation, Otake, Hiroshima 739-0652, Japan*
[2]*Mikuni-Makino Industrial Co., Ltd., Ashigarakami-gun, Kanagawa 258-0019, Japan*
[3]*Department of Physics, Shiga University of Medical Science, Otsu 520-2192, Japan*

In order to investigate the crystallization process of an $\alpha$-Fe/$Nd_2Fe_{14}B$ type nanocomposite magnet alloy, Mössbauer study has been carried out on $Nd_8Fe_{80}Co_4Nb_{1.5}B_{6.5}$ alloy ribbons prepared by melt spinning and post-heat-treatment at 600, 650, 700 and 760°C. The relative mass fractions of the $\alpha$-Fe, $Fe_3B$, $Nd_2Fe_{14}B$ and the intergranular phases, in crystallization process, were estimated from Mössbauer line-intensities. As-quenched alloys are practically amorphous states and start to crystallize at 600°C, but the crystallized grains are still so fine as to be observed with X-ray diffraction method and the Mössbauer spectroscopy. Around 650°C, $\alpha$-Fe, $Nd_2Fe_{14}B$ and metastable $Fe_3B$ phases are formed definitely and the amorphous phase decreases drastically but still remains as the intergranular phase. With increasing temperature, metastable $Fe_3B$ phase converts into $\alpha$-Fe, $Nd_2Fe_{14}B$, and a part of the intergranular phases also crystallize to form $\alpha$-Fe and $Nd_2Fe_{14}B$. At 760°C being the optimum heat-treating temperature to obtain the alloy with the best magnetic properties, about 10 mass% of the intergranular phases is considered to remain between the grains of $\alpha$-Fe and $Nd_2Fe_{14}B$.

(Received July 8, 2002; Accepted September 26, 2002)

***Keywords***: *Mössbauer study, $\alpha$-Fe, $Nd_2Fe_{14}B$, $Fe_3B$, amorphous, nanocomposite, exchange spring magnet, melt spinning*

## 1. Introduction

A so-called nanocomposite magnet alloy is composed of soft and hard magnetic grains on a nanometer scale. This alloy has a high remanence as well as a comparatively high coercivity due to the magnetic exchange coupling between the soft and hard magnetic grains. Therefore, the nanocomposite magnet alloy has been widely noticed as a hard magnetic material of the next generation.[1–10)]

Inoue *et al.*[11–15)] reported that, in the $\alpha$-Fe/$Nd_2Fe_{14}B$ type nanocomposite alloy, excess Nd atoms concentrated in the intergranular region cause the amorphous intergranular phase remaining even after heat-treatment, and result in inhibiting the grain growth and consequently improve magnetic properties. Our previous studies have shown that a small amount of Nb atoms added in the alloy plays the similar role as well.[16–20)] In these cases, the magnetic exchange coupling between the soft and hard phases should interacts through the intergranular ferromagnetic phase, which is supposed to be amorphous from the observation with X-ray and electron diffraction methods.

It is suggested by the micromagnetics theory that the magnetic exchange coupling through the intergranular phase plays a significant role in determining the magnetic properties.[21,22)] The intergranular phase, however, have hardly investigated so far in comparison with the soft and hard magnetic phases, because the intergranular phase is too thin to be analyzed by a method such as X-ray diffraction, *i.e.*, thinner than 5 nm.[19,20)] The three-dimensional atom probe (3DAP) analysis revealed that the Nb and excess B atoms are concentrated in the intergranular phase.[19,20)] Moreover, it is suggested by the 3DAP results that the distribution of atoms is not uniform in the intergranular phase. The Mössbauer analysis is most suitable for investigating the physical behavior of such a very thin layer as the intergranular phase in the present case, because it gives information on the nearest neighbor atoms of the prove element such as $^{57}Fe$.

The formation of the intergranular phase in the nanocomposite magnets should be crucially influenced by the quenching and heat-treating processes. The formation process of the alloys with the compositions of $Nd_7Fe_{88}B_5$ and $Nd_7Fe_{90}B_3$ was reported by Inoue *et al.* As the heat-treating temperature is increased, $\alpha$-Fe is crystallized at first, $Fe_3B$ follows and, at higher temperature, $Fe_3B$ is finally decomposed to convert $Nd_2Fe_{14}B$.[12)]

The present authors, Yamasaki and Hamano, obtained improved magnetic properties of $\alpha$-Fe/$Nd_2Fe_{14}B$ nanocomposite magnets by suitable heat treatment of the alloys containing a small amount of Nb and an excess of B which is partially crystallized just after the quenching.[16–18)] In the previous studies, however, they took no account of the metastable $Fe_3B$ phase in the crystallization process.

The purpose of this study is to investigate the details of the crystallization process. In order to follow the process, several heat-treated specimens were prepared, by changing the heat-treating temperature, from as-quenched alloys showing nearly amorphous state and were investigated with the Mössbauer spectroscopy.

## 2. Experimental

The melt-spun alloys with the composition $Nd_8Fe_{80}Co_4Nb_{1.5}B_{6.5}$ were prepared by the single roller melt-spinning process at a roll surface-velocity of 15 m/s in an Ar atmosphere. The crystallization process of the melt-spun ribbons, which were as quenched and heat-treated at 600, 650, 700 and 760°C, was followed by Mössbauer spectroscopy. The heat-treatment was done as follow. The ribbons were packed into quartz tube in vacuum at first, then they inserted into the heated furnace for 180 seconds and finally they were

taken out into water. The crystallization state of the ribbon was confirmed by X-ray diffraction (Fe-K$\alpha$). The magnetic measurements were carried out by using a vibrating sample magnetometer (VSM). The specimens for Mössbauer spectroscopy were prepared by milling the ribbon and sieving under 90 μm. The Mössbauer measurements were carried out in the conventional transmission mode at room temperature with a $^{57}$Co source of about 740 MBq.

## 3. Results and Discussions

### 3.1 X-ray diffraction spectra

The X-ray diffraction patterns of the ribbon alloys heat-treated at various temperatures are shown in Fig. 1. The pattern of the ribbon heat-treated at 500°C is quite similar to that of the as-quenched ribbon, and both patterns have broad banks probably due to the phase structure being at an almost amorphous state. The diffraction peaks around 54° and 57° due to $\alpha$-Fe, $Fe_3B$ or $Nd_2Fe_{14}B$ start to appear from 600°C. It is, however, difficult to say which phase in the ribbon is responsible to the peaks because they are weak and broad reflecting fine size of the grains.

The intensity of the diffraction peak around 54° due to $Fe_3B$ increases significantly at 650°C and another new diffraction peak due to $Fe_3B$ appears around 61°. The peaks around 57° and at 40–50° due to $Nd_2Fe_{14}B$ also grow up. From the above results, it can be said that $\alpha$-Fe, $Fe_3B$ and $Nd_2Fe_{14}B$ start to be crystallized collectively at 650°C.

The diffraction peaks due to $Nd_2Fe_{14}B$ grow up significantly at 700°C and another peak at 61–62° appears beside that of $Fe_3B$. The peak due to $\alpha$-Fe also grows up. In contrast, the diffraction peaks due to $Fe_3B$ reduce slightly at 700°C, and these peaks continue to reduce at higher temperatures, and then eventually disappear at 760°C.

The analysis of Mössbauer spectra was carried out based on these experimental results.

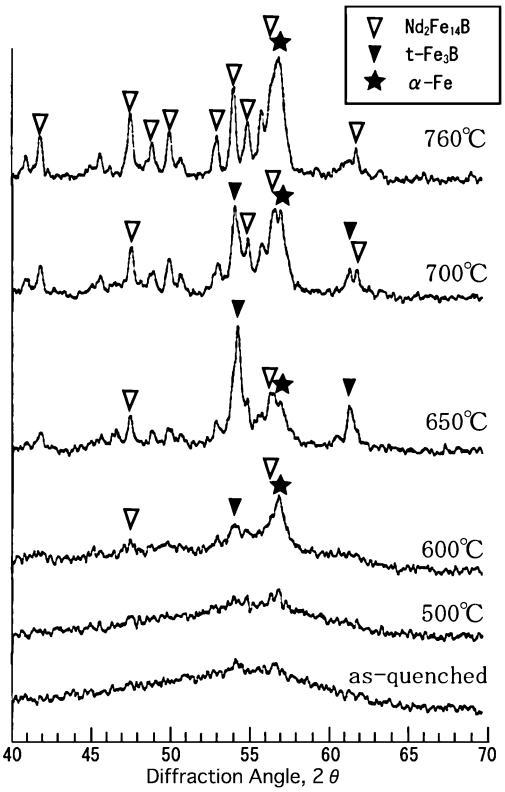


Fig. 1 The X-ray diffraction patterns of $Nd_8Fe_{80}Co_4Nb_{1.5}B_{6.5}$ melt-spun ribbon alloys heat-treated at various temperatures.

### 3.2 Mössbauer analysis

#### 3.2.1 Amorphous phase (as-quenched and heat-treated at 600°C)

As shown in Fig. 2, the Mössbauer spectra of two specimens, as-quenched and heat-treated at 600°C, are quite similar to those of typical amorphous alloys as expected from the X-ray diffraction patterns. There is almost no long-range magnetic order in alloys, and the magnetic hyperfine field may distribute broadly.

The Mössbauer spectrum of the as-quenched alloy was first analyzed by supposing one component with a hyperfine-field distribution. The calculated spectrum, however, did not fit well to the observed one. In order to reproduce a satisfactory

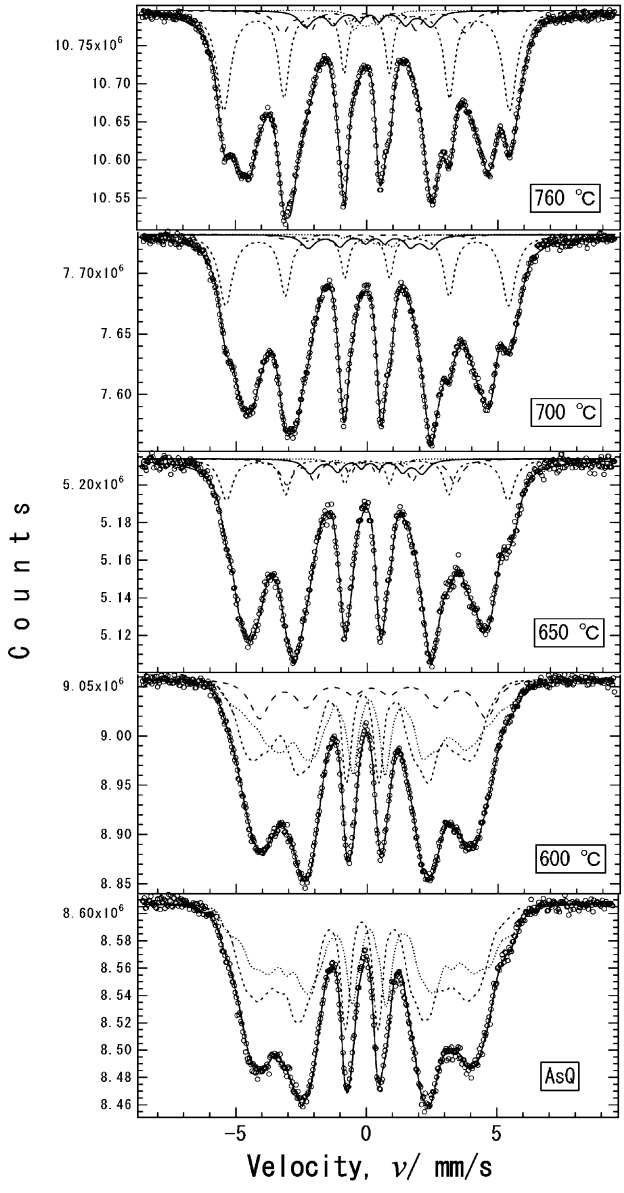


Fig. 2 The Mössbauer spectra of $Nd_8Fe_{80}Co_4Nb_{1.5}B_{6.5}$ melt-spun ribbon alloys heat-treated at various temperatures.

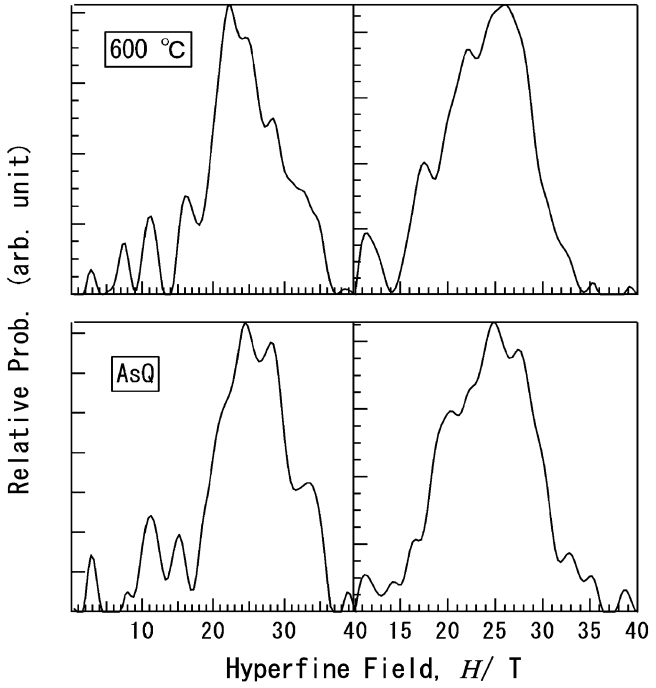


Fig. 3 The hyperfine-field distributions obtained from the spectra of the alloys as-quenched and heat-treated at 600°C.

spectrum, at least two distributions have to be supposed; one has a positive isomershift and the other has a negative one.

In the case of the alloy heat-treated at 600°C, several sextets corresponding to $\alpha$-Fe, $Nd_2Fe_{14}B$ or $Fe_3B$ were supposed, at first, besides two components with hyperfine-field distribution for the analysis of the spectrum, but no reasonable result was obtained. The crystal grains at this temperature are too fine to form Mössbauer lines characteristic of the above-mentioned phases in the spectrum. The spectrum at 600°C was analyzed, therefore, by supposing one sextet in addition to two components with field distribution.

The hyperfine-field distributions obtained from the spectra of the alloys as-quenched and heat-treated at 600°C are shown in Fig. 3. The isomershifts of the components with the left and right distributions in the figure are positive and negative, respectively. The hyperfine-field distributes broadly around approximately 25 T, which is smaller than the hyperfine field of $\alpha$-Fe, *i.e.*, 33 T, but not so small as to be paramagnetic. This suggests there is local short-range magnetic order in the alloys. The distributions of the two alloys in Fig. 3 are similar well with each other, which supports the above assumptions for the analysis of the spectra.

Considering the X-ray diffraction peaks, the sextet in the spectrum at 600°C is probably due to $Nd_2Fe_{14}B$ or $\alpha$-Fe.

### 3.2.2 The crystallization (heat-treated at 650, 700, 760°C).

In the analysis of the Mössbauer spectra of the alloys heat-treated at 650, 700 and 760°C, the contribution of $\alpha$-Fe, $Nd_2Fe_{14}B$ and $Fe_3B$ to the spectra was taken into account with the following assumptions. The relative-intensity ratios of the sextets were assumed to be 3:2:1:1:2:3, that is, a random orientation of nanocrystalline grains was assumed. The widths of all sextets were assumed the same. The isomer-shift ($\delta$) and quadrupole-splitting ($\Delta$) of $\alpha$-Fe were fixed to zero mm/s

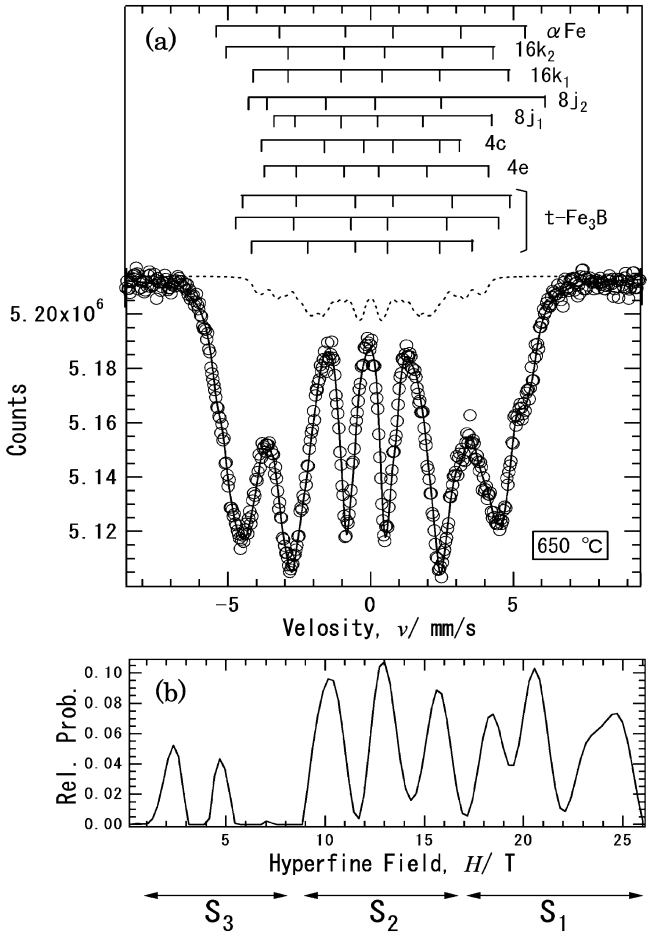


Fig. 4 Mössbauer spectrum and analyzed results for $Nd_8Fe_{80}Co_4Nb_{1.5}B_{6.5}$ melt-spun ribbon alloys heat-treated at 650°C. Above the spectrum (a), the line positions of the sextets due to $\alpha$-Fe, $Nd_2Fe_{14}B$ and t-$Fe_3B$ are given in the diagrams, the component with hyperfine-field distribution corresponding to the phase other than $\alpha$-Fe, $Nd_2Fe_{14}B$ and t-$Fe_3B$ is represented by a broken line in the spectrum, the field distribution of which is shown in (b).

referring to $\alpha$-Fe metal at room temperature. The intensity ratios of the components corresponding to the Fe sites $16k_2$, $16k_1$, $8j_2$, $8j_1$, 4c and 4e in the $Nd_2Fe_{14}B$ phase were fixed to 16:16:8:8:4:4 according to the ratio of Fe occupancy.

There are three Fe sites in $Fe_3B$ phase[25] and, in this study, the ratios of line-intensity of the Fe sites in the $Fe_3B$ phase were assumed as 1:1:1 in proportion to the number of Fe sites. It was reported that the intensity ratio of $Fe_3B$ in bulk is different from 1:1:1,[25] but the situation in the present study is quite different from that of the bulk case: the crystal growth is insufficient and/or the grains are fine. In the present study, we can, therefore, find no definite reason to shift the ratio from 1:1:1.

The observed Mössbauer spectra can be simulated by assuming a magnetic component with a hyperfine-field distribution besides the sextet components of $\alpha$-Fe, $Nd_2Fe_{14}B$ and $Fe_3B$, an example of which is shown in Fig. 4. As can be seen from the figure, several definite peaks are noticed in the distribution, which suggests that the phase reflecting to this distribution is not typical amorphous. As considered in our previous study,[24] the component with this distribution may represent the several layers on the surface of grains of $\alpha$-Fe, $Nd_2Fe_{14}B$ and $Fe_3B$. For convenience, three compo-

Table 1 Obtained Mössbauer parameters of $Nd_8Fe_{80}Co_4Nb_{1.5}B_{6.5}$ melt-spun ribbon alloys heat-treated at various temperatures. $\delta$ and $\Delta$ refer to $\alpha$-Fe metal at room temperature.

| Alloy | Phase | Site | $\delta$ (mm/s) | $\Delta$ (mm/s) | Hyperfine field (T) | | Relative intensity (%) |
|---|---|---|---|---|---|---|---|
| As-Q | S3_1 | | 0.14 | 0.06 | | | 45.5 |
| | S3_2 | | −0.16 | 0.03 | | | 54.5 |
| 600°C | some crystal | | 0.19 | 0.06 | 26.8 | | 14.2 |
| | S3_1 | | 0.11 | 0.07 | | | 41.6 |
| | S3_2 | | −0.21 | −0.07 | | | 44.2 |
| 650°C | $\alpha$-Fe | | 0.00 | 0.00 | 33.3 | | 9.8 |
| | $Nd_2Fe_{14}B$ | $16k_2$ | −0.29 | −0.10 | 28.7 | | 49.8 |
| | | $16k_1$ | 0.01 | 0.34 | 27.8 | | |
| | | $8j_2$ | 0.11 | 0.81 | 31.9 | | |
| | | $8j_1$ | 0.01 | 0.42 | 23.4 | | |
| | | 4c | −0.03 | −0.39 | 21.5 | | |
| | | 4e | −0.11 | 0.21 | 24.6 | | |
| | S1 | | 0.00 | 0.29 | 20.0 | 5.9 | 10.3 |
| | S2 | | 0.03 | −0.15 | 13.2 | 3.4 | |
| | S3 | | 0.07 | −0.15 | | 1.0 | |
| | $Fe_3B$ | | 0.19 | 0.03 | 29.0 | | 30.0 |
| | | | −0.08 | −0.09 | 28.6 | | |
| | | | −0.07 | −0.16 | 24.1 | | |
| 700°C | $\alpha$-Fe | | 0.00 | 0.00 | 33.5 | | 17.6 |
| | $Nd_2Fe_{14}B$ | $16k_2$ | −0.17 | −0.12 | 27.9 | | 58.4 |
| | | $16k_1$ | −0.05 | 0.42 | 28.5 | | |
| | | $8j_2$ | 0.07 | 0.65 | 33.0 | | |
| | | $8j_1$ | 0.06 | 0.50 | 26.4 | | |
| | | 4c | −0.32 | −1.14 | 25.8 | | |
| | | 4e | −0.21 | 0.02 | 25.0 | | |
| | S1 | | 0.03 | 0.67 | 22.2 | 1.0 | 5.6 |
| | S2 | | 0.19 | −0.23 | 14.4 | 3.3 | |
| | S3 | | 0.50 | −0.26 | | 1.3 | |
| | $Fe_3B$ | | 0.17 | 0.01 | 27.4 | | 18.3 |
| | | | 0.03 | 0.21 | 23.6 | | |
| | | | 0.07 | 0.14 | 20.7 | | |
| 760°C | $\alpha$-Fe | | 0.00 | 0.00 | 33.7 | | 25.2 |
| | $Nd_2Fe_{14}B$ | $16k_2$ | −0.11 | −0.05 | 28.9 | | 63.4 |
| | | $16k_1$ | −0.04 | 0.45 | 28.6 | | |
| | | $8j_2$ | 0.04 | 0.61 | 33.6 | | |
| | | $8j_1$ | −0.01 | 0.30 | 25.2 | | |
| | | 4c | −0.17 | −0.89 | 24.4 | | |
| | | 4e | −0.10 | 0.00 | 25.3 | | |
| | S1 | | 0.17 | 0.41 | 21.6 | 5.7 | 11.4 |
| | S2 | | 0.08 | −0.04 | 114.7 | 4.0 | |
| | S3 | | 0.11 | 0.33 | | 1.7 | |

nents, S1, S2 and S3, were assumed to be representative in the field ranges of 17–26 T, 9–17 T and below 9 T, respectively, as shown in Fig. 4(b). The last component S3 was assumed to represent a practically amorphous phase. The Mössbauer spectra were, then, decomposed into Lorentzian sextets of $\alpha$-Fe, $Nd_2Fe_{14}B$, $Fe_3B$, S1, S2 and a component with a hyperfine-field distribution S3. The obtained parameters were listed in Table 1 and show a good agreement with those described in other studies.[25)]

From the relative intensities of components in the Mössbauer spectra shown in Table 1, the relative mass fractions (mass%) of $\alpha$-Fe, $Nd_2Fe_{14}B1$, $Fe_3B$ and S = (S1+S2+S3) in the alloys are estimated. Here, all of the phases S1, S2 and S3 are brought together to the item of amorphous phase that composed only of Fe, Nb and excess B atoms. The mass fractions estimated in this way are shown in Fig. 5.

As seen in Fig. 5, only about 15% of atoms in the alloy heat-treated at 600°C starts to crystallize, but the grains grow insufficiently and we cannot say in which phase of $\alpha$-Fe, $Nd_2Fe_{14}B$ and $Fe_3B$ the grains are. The other part of the alloy is amorphous or nearly amorphous. At 650°C, this amorphous phase decreases drastically down to about 10% and the grains with the above three phases $\alpha$-Fe, $Nd_2Fe_{14}B$ and $Fe_3B$ are formed definitely. The relative mass fraction of the metastable $Fe_3B$ is greatest at 650°C, decreases at higher temperature and disappears practically at 760°C. The fractions of $\alpha$-Fe and $Nd_2Fe_{14}B$ increase at higher temperature at the cost of $Fe_3B$ and amorphous S phases. In these processes, a lot of B is released in the alloy and promotes the formation of the S phase, which may be the reason why the S phase

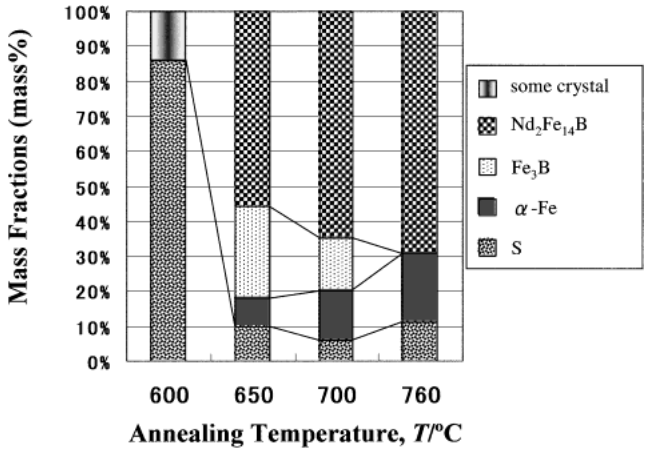


Fig. 5 The mass fractions estimated from the hyperfine-field distribution of $Nd_8Fe_{80}Co_4Nb_{1.5}B_{6.5}$ melt-spun ribbon alloys heat-treated at various temperatures.

increases again at 760°C.

## 4. Conclusion

On melt spun alloy of $\alpha$-Fe/$Nd_2Fe_{14}B$ type $Nd_8Fe_{80}Co_4Nb_{1.5}B_{6.5}$ nanocomposite magnet, the relative mass fractions of the $\alpha$-Fe, $Fe_3B$, $Nd_2Fe_{14}B$ and intergranular phases, in crystallization process, were estimated with the Mössbauer spectroscopy.

A practically amorphous alloy as quenched starts to crystallize at 600°C in the heat-treating process, but the crystallized grains are too fine to be observed with the X-ray diffraction method and Mössbauer spectroscopy. Around 650°C $\alpha$-Fe, $Nd_2Fe_{14}B$ and metastable $Fe_3B$ phase are formed definitely, and the amorphous phase decreases drastically but still remains as S1–S3 phases. With increasing temperature, metastable $Fe_3B$ phase convert into $\alpha$-Fe, $Nd_2Fe_{14}B$ and a part of the S1–S3 phases crystallizes also to form $\alpha$-Fe and $Nd_2Fe_{14}B$. At 760°C being the optimum heat-treating temperature to obtain the alloy with the best magnetic properties, about 10 mass% of S1–S3 remains as the intergranular phase between the grains of $\alpha$-Fe and $Nd_2Fe_{14}B$.

## REFERENCES


1) K. H. J. Buschow, D. B. DeMooij and R. Coehoorn: J. Less-Common Met. **145** (1988) 601–611.
2) E. F. Kneller and R. Hawig: IEEE Trans. Magn. **MAG-27** (1991) 3588–3600.
3) T. Schrefl, H. Kronmuller and J. Fidler: J. Magn. Magn. Mater. **127** (1993) L273–L277.
4) R. Skomski and J. M. D. Coey: Phys. Rev. **B48** (1993) 15812–15816.
5) A. Manaf, R. A. Buckly and H. A. Davis: J. Magn. Magn. Mater. **128** (1993) 302–306.
6) S. Hirosawa, H. Kanekiyo and M. Uehara: J. Appl. Phys. **73** (1993) 6488–6490.
7) R. Skomski: J. Appl. Phys. **76** (1994) 7059–7064.
8) J. M. Yao, T. S. Chin and S. K. Chen: J. Appl. Phys. **76** (1994) 7071–7073.
9) L. Withanawassam, A. S. Murphy, G. C. Hadjipanysis and R. F. Krause: J. Appl. Phys. **76** (1994) 7065–7067.
10) V. Panchanathan: IEEE Trans. Magn. **31-6** (1995) 3605–3607.
11) A. Inoue, A. Takeuchi, A. Makino and T. Masumoto: IEEE Trans. Magn. **31-6** (1995) 3626–3628.
12) A. Inoue, A. Takeuchi, A. Makino and T. Masumoto: Mater. Trans., JIM **36** (1995) 676–687.
13) A. Inoue, A. Takeuchi, A. Makino and T. Masumoto: Mater. Trans., JIM **36** (1995) 962–971.
14) A. Inoue, A. Takeuchi, A. Makino and T. Masumoto: Sci. Rep. RITU **A42-1** (1996) 143–156.
15) A. Takeuchi, A. Inoue and A. Makino: Mater. Sci. and Engin. **A226–228** (1997) 458–462.
16) M. Hamano, M. Yamasaki, H. Mizuguchi, H. Yamamoto and A. Inoue: Proc. 15th International Workshop on Rare-earth Magnets, Dresden, 30 Aug.–3 Sep., Vol. 1 (1998) 199–204.
17) M. Yamasaki, H. Mizuguchi, M. Hamano, H. Yamamoto and A. Inoue: T. IEE Japan **119-A** (1999) 790–795.
18) M. Hamano, M. Yamasaki, H. Mizuguchi, T. Kobayashi, H. Yamamoto and A. Inoue: Mat. Res. Soc. Symp. Proc. **577** (1999) 187–194.
19) Y. Q. Wu, D. H. Ping, K. Hono and A. Inoue: IEEE Trans. Magn. **35** (1999) 3295–3297.
20) Y. Q. Wu, D. H. Ping, K. Hono M. Hamano and A. Inoue: J. Appl. Phys. **87** (2000) 8658–8665.
21) H. Fukunaga, J. Kuma and Y. Kanai: IEEE Trans. Magn. **35** (1999) 3235–3240.
22) T. Schrefl, J. Fidler and D. Süss: Proc. 11th int. Symposium on Magnetic Anisotropy and Coercivity in RE-TM alloys (2000) S57–S71.
23) L. Withanawassam, G. C. Hadjipanysis and R. F. Krause: J. Appl. Phys. **75** (10) (1994) 6646–6648.
24) T. Kobayashi, M. Yamasaki and M. Hamano: J. Appl. Phys. **87** (2000) 6579–6581.
25) T. Hinomura, S. Nasu, H. Kanekiyo and S Hirosawa: J. Japan Inst. Metals. **61** (1997) 184–190.